Journal of Clinical Neuroscience 23 (2016) 63–67

Contents lists available at ScienceDirect

Journal of Clinical Neuroscience

journal homepage: www.elsevier.com/locate/jocn

Clinical Study

Effect of endoscopic third ventriculostomy on cerebrospinal fluid pressure in the cerebral ventricles

Azadeh Farnoush [a], Kristy Tan [b,c], Lauriane Juge [b,e], Lynne E. Bilston [b,d], Shaokoon Cheng [a,b,*]

[a] Faculty of Science and Engineering, Macquarie University, NSW, Australia
[b] Neuroscience Research Australia, Randwick, NSW, Australia
[c] Graduate School of Biomedical Engineering, University of New South Wales, NSW, Australia
[d] Prince of Wales Clinical School, University of New South Wales, NSW, Australia
[e] School of Medical Sciences, University of New South Wales, Sydney, NSW, Australia

ARTICLE INFO

Article history:
Received 20 March 2015
Accepted 11 April 2015

Keywords:
Cerebrospinal fluid
Cerebral ventricles
Computational fluid dynamics
Endoscopic third ventriculostomy
Hydrocephalus

ABSTRACT

We aimed to show how endoscopic third ventriculostomy (ETV) treatment may affect cerebrospinal fluid (CSF) flow dynamics in hydrocephalus, with and without aqueductal stenosis. Hydrocephalus is a neurological disorder which is characterized by enlarged brain ventricles. The periodic motion of CSF flow as a function of the cardiac cycle was prescribed as the inlet boundary condition at the foramen of Monro, and ETV was modeled as a 5 mm diameter hole in the anterior wall of the third ventricle. The results show that ETV reduces the pressure in the ventricles by nine-fold in the model with aqueductal stenosis, and three-fold in the model without aqueductal stenosis. More importantly, ETV changes the temporal characteristics of the CSF pressure waveform in the model without aqueductal stenosis, such that there is higher pressure in the ventricle during diastole. This study suggests that changes in the temporal characteristics of the CSF pressure waveform in the ventricles may be the reason why ETV treatment is not effective for hydrocephalus without aqueductal stenosis.

1. Introduction

Hydrocephalus is a structural neurological disorder which is marked by enlarged brain ventricles with complex pathophysiology, and can develop with or without frank obstruction to cerebrospinal fluid (CSF) flow. The mechanisms of ventricular enlargement in hydrocephalus remain unclear, and are likely related to an increase in small pulsatile pressure [1,2] instead of a large transmantle pressure gradient between the ventricles and subarachnoid spaces [3].

The CSF pulsatile pressure in the ventricles is related to the dynamic relationship between CSF and cerebral blood flow, and this has been clearly demonstrated in MRI studies [4]. As the cranium is rigid, during cardiac systole, blood flow into the cranium is compensated for by the translocation of CSF from the subarachnoid spaces and lateral ventricles. An increased blood flow in the brain results in minute brain expansion, which also causes a decrease in cerebral ventricular volume, in particular within the lateral ventricles [4]. Therefore, during systole, the slight compression on the ventricles increases CSF pressure and this pushes CSF out of the ventricles through the cerebral aqueduct. During diastole, CSF flows rostrally to refill the cerebral ventricles as cerebral blood leaves the cranium.

The primary treatment for hydrocephalus involves the diversion of CSF from the cerebral ventricles to the atrial or peritoneal cavity using a mechanical shunt implant. Shunt devices have high failure rates [5] and implantations and revisions cost approximately $1 billion/year in the USA [6]. Endoscopic third ventriculostomy (ETV) is an alternative treatment for hydrocephalus which involves the diversion of CSF from the cerebral ventricles via a surgical bypass at the floor of the third ventricle. Although ETV is a promising treatment, as it does not require any implants, the effectiveness of this treatment varies between patients. For example, ETV is known to be effective in patients with aqueductal stenosis, but less effective in patients with non-obstructive hydrocephalus [7]. The reason for this is unclear and may be related to differences in CSF flow dynamics when ETV is performed in hydrocephalus patients with different degrees of obstruction to CSF flow.

We aimed to show how ETV affects CSF flow dynamics in hydrocephalus models by using computational fluid dynamics (CFD). We hypothesized that ETV changes the temporal characteristics of the CSF pressure waveform in different ways in hydrocephalus ventricles with aqueductal stenosis (HAS) and without (HNAS).

* Corresponding author. Tel.: +61 2 9580 9063.
E-mail address: shaokoon.cheng@mq.edu.au (S. Cheng).

http://dx.doi.org/10.1016/j.jocn.2015.04.025
0967-5868/

2. Methods

A 3D model of the cerebral ventricle was constructed using a set of high resolution anatomical axial and coronal MRI (pixel resolution of 1 mm) collected from an adult patient with HNAS. This was achieved by manually outlining the cross-sections of the ventricles and cerebral aqueduct on the MRI, and representing these with volumetric splines (Surfdriver software; version 3.5). These splines were exported to Rhinoceros (version 3; Robert McNeel and Associates, Seattle, WA, USA) for construction of the surfaces of the ventricles and the cerebral aqueduct (Fig. 1).

To provide a meaningful and direct comparison between the HAS and HNAS models, the geometry of the two models was quasi-identical. The only difference between the models was that the cross-sectional area at the midlevel of the cerebral aqueduct in the HAS model was 50% smaller than the HNAS model.

ETV was modeled as a 5 mm diameter hole in the anterior wall of the third ventricle [8]. Therefore, four different models were generated for this study: HAS with and without ETV and HNAS with and without ETV (Table 1). The models were meshed with unstructured tetrahedral elements using the commercial package Ansys CFX (version 14.0, ANSYS, Canonsburg, PA, USA) and higher mesh density was created at the foramen of Monro (FOM) and the cerebral aqueduct. All models were ensured to be within 0.1 mm of the original segmented MRI data.

Ansys CFX was used to perform CFD analysis by solving the Navier–Stokes equations for an incompressible fluid with a constant viscosity. The finite volume approach was applied to solve these equations and second order differencing was used in both space and time. The simulations were performed by first solving for steady flow at the flux, corresponding to the time zero value. Then, for transient simulations, a time varying flow was prescribed at the inlet. Multiple time steps were trialed to ensure time independence of the solutions, and iterations were performed at each time step to ensure that the normalized residuals were less than 10^{-4}. Mesh sensitivity was also performed by considering three different discretization schemes, as shown in Table 2. The estimation of the relative error of the flow rate introduced by grid and time discretization was calculated at the center of the cerebral ventricles in the model, using the following formula [9]:

$$e = \max\left(\left|\frac{Q_{fine} - Q_{medium}}{Q_{fine}}\right|\right) \times 100$$

The relative error of less than 5% confirmed that the minimum grid (214,604) and time step (0.01) used in the models did not affect the accuracy of the solutions.

Table 1
Configuration of the four different models generated for this study with prescribed boundary conditions

Model	Type of hydrocephalus	ETV	Foramen of Monro		ETV incision
			Inlet boundary condition	Outlet boundary condition	Outlet boundary condition
1	HAS	N	Velocity*	Pressure at 0 Pa	No ETV
2	HAS	Y	Velocity*	Pressure at 0 Pa	Pressure at 0 Pa
3	HNAS	N	Velocity*	Pressure at 0 Pa	No ETV
4	HNAS	Y	Velocity*	Pressure at 0 Pa	Pressure at 0 Pa

ETV = endoscopic third ventriculostomy, HAS = hydrocephalus with aqueductal stenosis, HNAS = hydrocephalus without aqueductal stenosis, N = no, Y = yes.
* Velocity was prescribed at inlet as a function of cardiac cycle.

Table 2
Details of the parameters used to test time and grid independence of the solutions

	Grid independence		Time step independence	
	Elements, n	Relative error* compared to 1, %	Time steps	Relative error* compared to 1, %
1	214,604	-	0.01	-
2	586,133	<5%	0.001	<5%
3	1,233,464	<5%	0.0001	<5%

* Estimation of relative error introduced by spatial and temporal discretization.

CSF was modelled as an incompressible Newtonian fluid with a dynamic viscosity of 1.0 mPa.s (millipascal seconds) [10]. CSF flow was laminar, as Reynolds number (Re) was checked for all parts of the ventricles and no turbulent effects were found (Re < 100). No slip-boundary conditions were applied on the surfaces of the ventricles. The CSF velocity in the FOM was obtained by matching the reported measurements of CSF velocity in the cerebral aqueduct of a typical HNAS patient [11]. The CSF velocity at the FOM was then prescribed as an inlet boundary condition in all models. All pressures are reported relative to pressure at the caudal end of the FOM and at the ETV outlet.

3. Results

The simulated CSF velocity in the cerebral aqueduct in the models without ETV corresponded well with the values that are

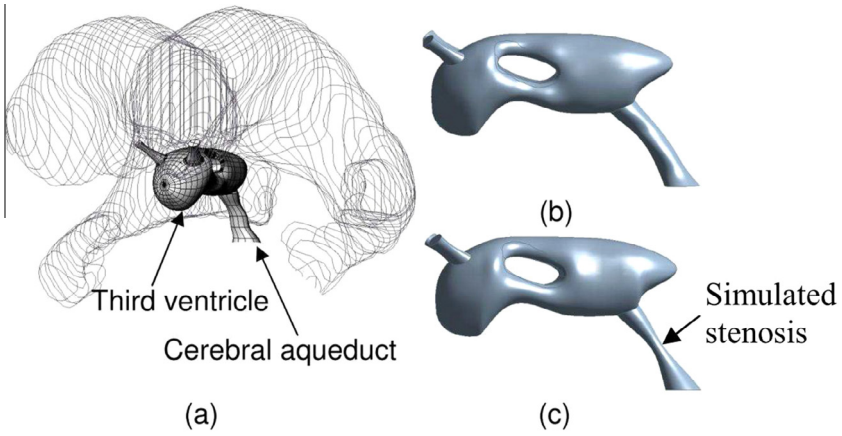

Fig. 1. (a) Geometry of the base 3D computational model, including third ventricle and cerebral aqueduct reconstructed from the MRI; (b) hydrocephalus third ventricle without aqueductal stenosis; (c) hydrocephalus third ventricle with aqueductal stenosis.